Neuron, Volume *93*

Supplemental Information

A Brainstem-Spinal Cord Inhibitory Circuit for Mechanical Pain Modulation by GABA and Enkephalins

Amaury François, Sarah A. Low, Elizabeth I. Sypek, Amelia J. Christensen, Chaudy Sotoudeh, Kevin T. Beier, Charu Ramakrishnan, Kimberly D. Ritola, Reza Sharif-Naeini, Karl Deisseroth, Scott L. Delp, Robert C. Malenka, Liqun Luo, Adam W. Hantman, and Grégory Scherrer

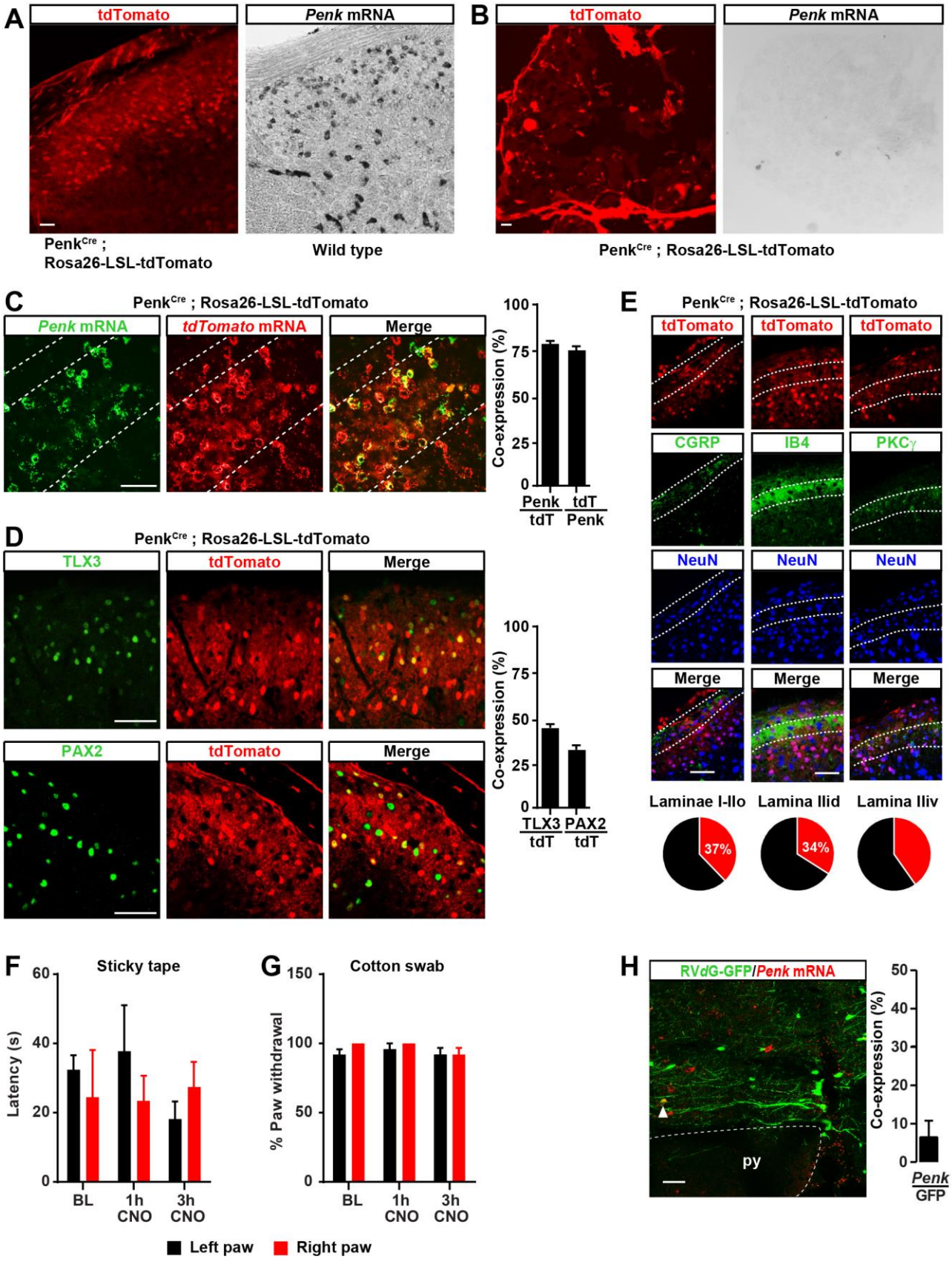
A
tdTomato
Penk mRNA
Penk^Cre ; Rosa26-LSL-tdTomato
Wild type
B
tdTomato
Penk mRNA
Penk^Cre ; Rosa26-LSL-tdTomato
C
Penk^Cre ; Rosa26-LSL-tdTomato
Penk mRNA
tdTomato mRNA
Merge
Co-expression (%)
100
75
50
25
0
Penk / tdT
tdT / Penk
D
Penk^Cre ; Rosa26-LSL-tdTomato
TLX3
tdTomato
Merge
PAX2
tdTomato
Merge
Co-expression (%)
100
75
50
25
0
TLX3 / tdT
PAX2 / tdT
E
Penk^Cre ; Rosa26-LSL-tdTomato
tdTomato
tdTomato
tdTomato
CGRP
IB4
PKCγ
NeuN
NeuN
NeuN
Merge
Merge
Merge
Laminae I-IIo
Lamina IIid
Lamina IIiv
37%
34%
F
Sticky tape
Latency (s)
60
40
20
0
BL
1h CNO
3h CNO
G
Cotton swab
% Paw withdrawal
150
100
50
0
BL
1h CNO
3h CNO
Left paw
Right paw
H
RVdG-GFP/Penk mRNA
py
Co-expression (%)
50
40
30
20
10
0
Penk / GFP

Figure S1

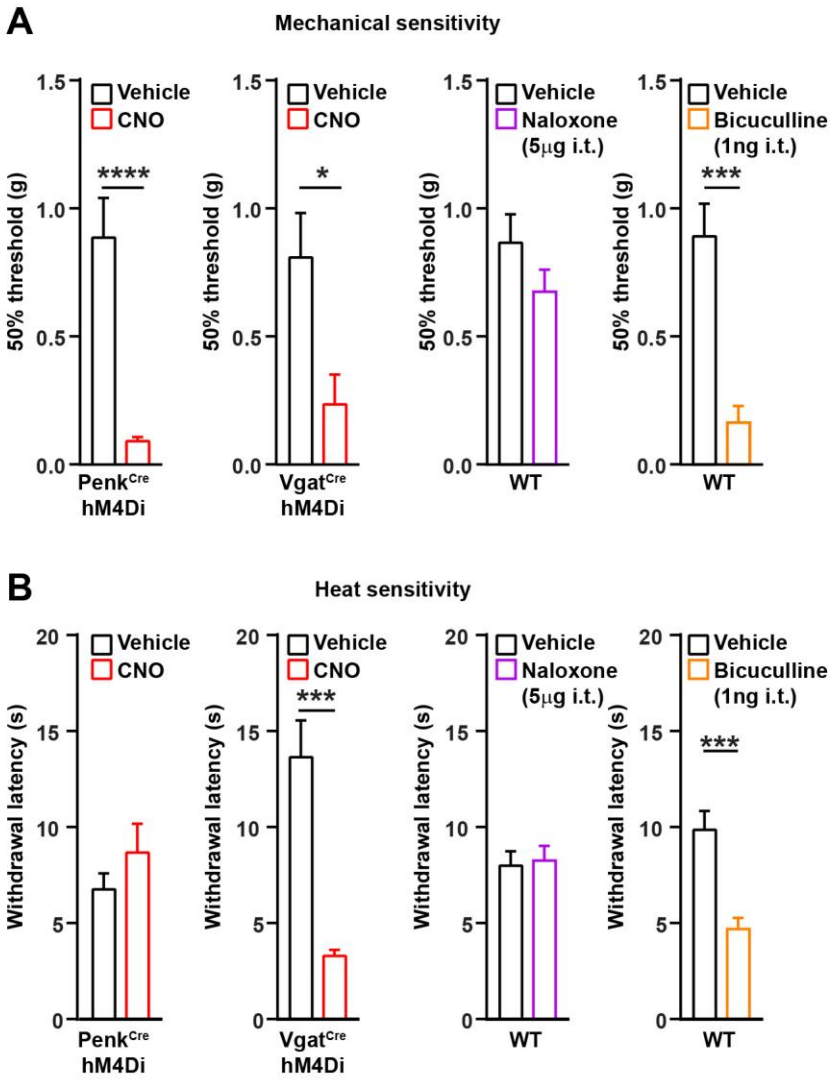
A
Mechanical sensitivity
50% threshold (g)
Vehicle
CNO
****
Penk^Cre hM4Di
*
Vgat^Cre hM4Di
Naloxone (5μg i.t.)
WT
Bicuculline (1ng i.t.)
***
B
Heat sensitivity
Withdrawal latency (s)

Figure S2

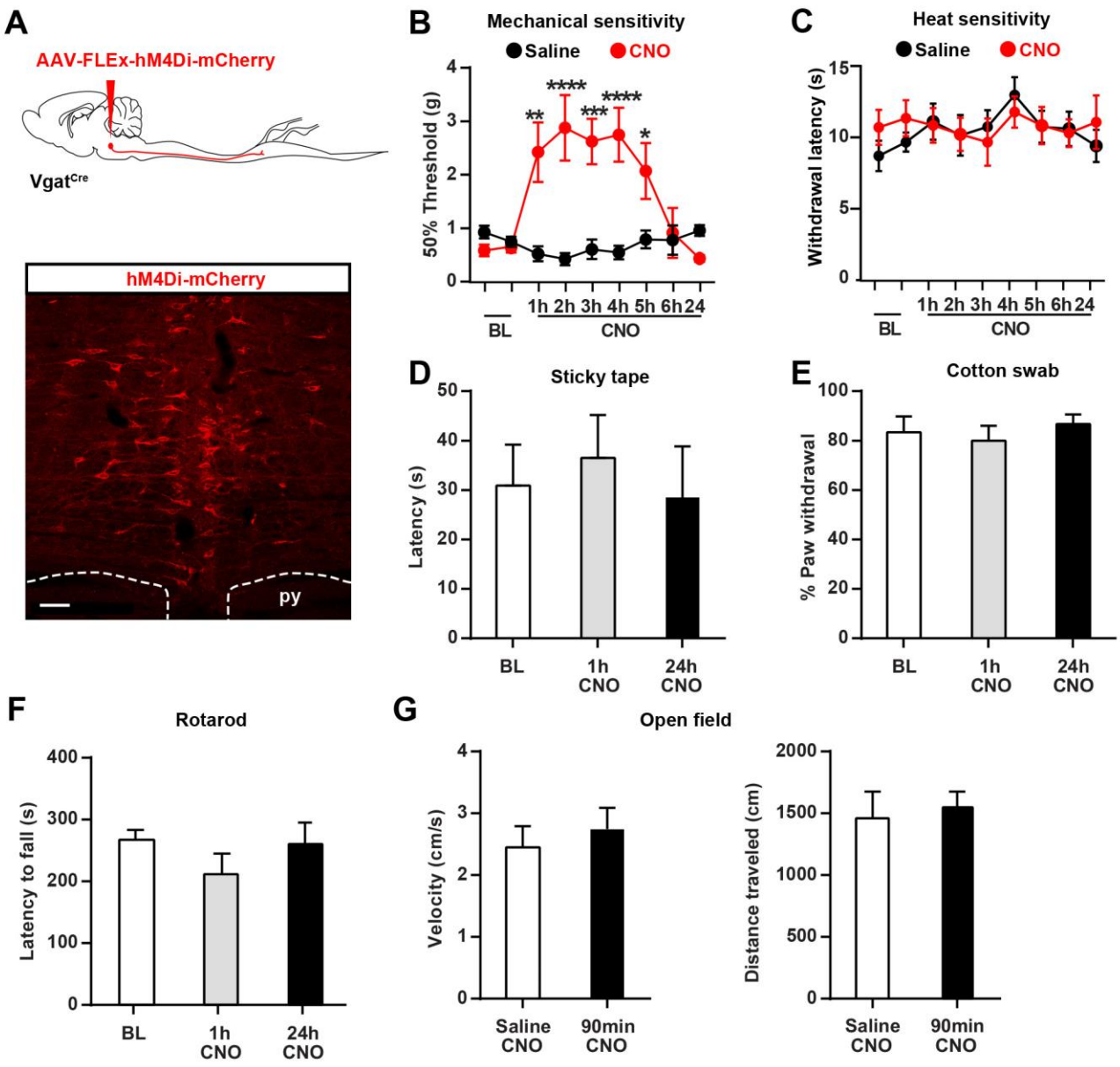
A
AAV-FLEx-hM4Di-mCherry
Vgat^Cre
hM4Di-mCherry
py
B
Mechanical sensitivity
Saline
CNO
50% Threshold (g)
**
****
***
****
*
1h 2h 3h 4h 5h 6h 24
BL
CNO
C
Heat sensitivity
Saline
CNO
Withdrawal latency (s)
1h 2h 3h 4h 5h 6h 24
BL
CNO
D
Sticky tape
Latency (s)
BL
1h CNO
24h CNO
E
Cotton swab
% Paw withdrawal
BL
1h CNO
24h CNO
F
Rotarod
Latency to fall (s)
BL
1h CNO
24h CNO
G
Open field
Velocity (cm/s)
Saline CNO
90min CNO
Distance traveled (cm)
Saline CNO
90min CNO

Figure S3

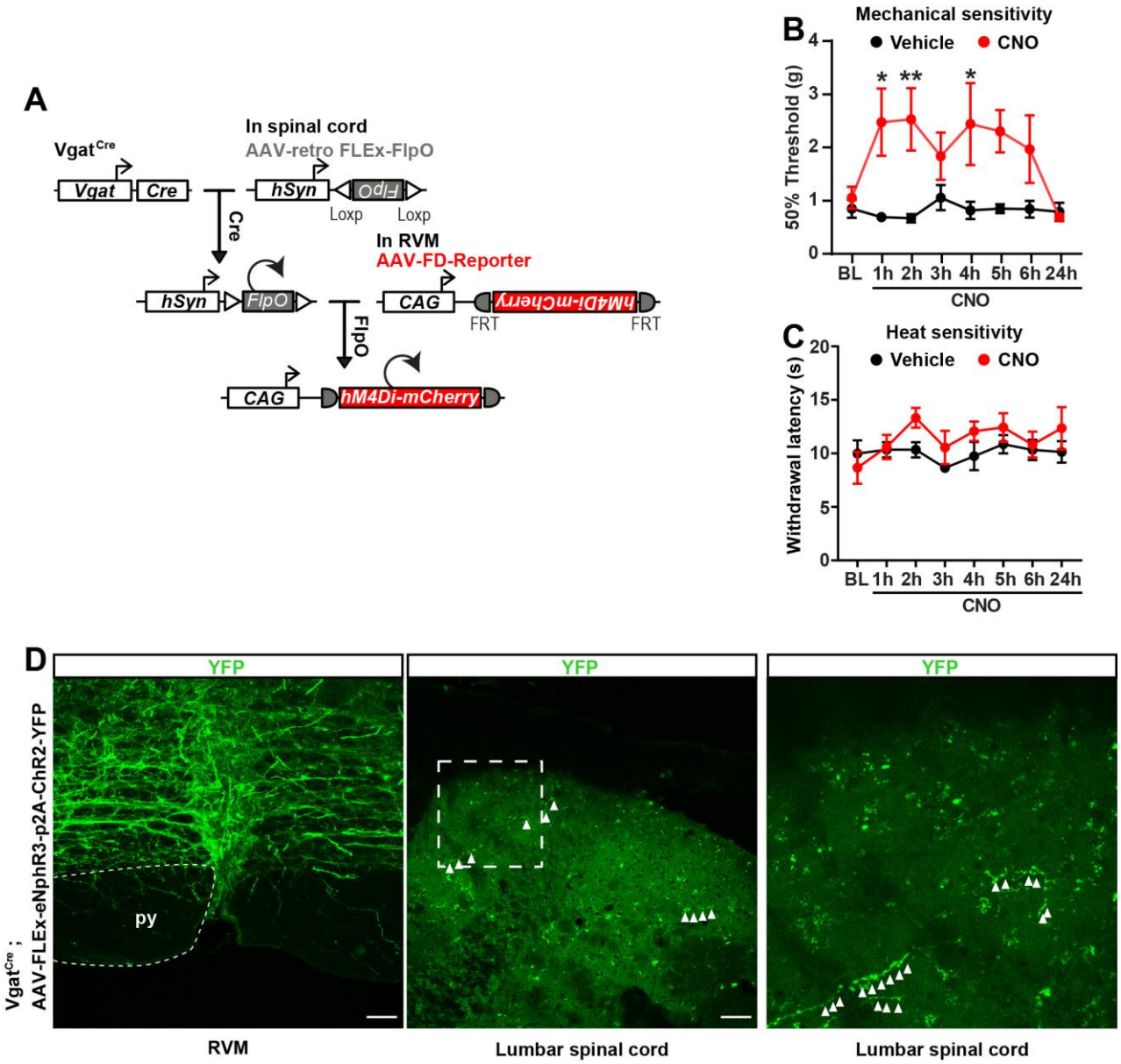
A
In spinal cord
AAV-retro FLEx-FlpO
Vgat Cre
Vgat Cre
hSyn FlpO
Loxp Loxp
Cre
In RVM
AAV-FD-Reporter
hSyn FlpO
CAG hM4Di-mCherry
FRT FRT
FlpO
CAG hM4Di-mCherry
B
Mechanical sensitivity
Vehicle CNO
50% Threshold (g)
BL 1h 2h 3h 4h 5h 6h 24h
CNO
C
Heat sensitivity
Vehicle CNO
Withdrawal latency (s)
BL 1h 2h 3h 4h 5h 6h 24h
CNO
D
YFP
YFP
YFP
Vgat Cre ; AAV-FLEx-eNphR3-p2A-ChR2-YFP
py
RVM
Lumbar spinal cord
Lumbar spinal cord

Figure S4

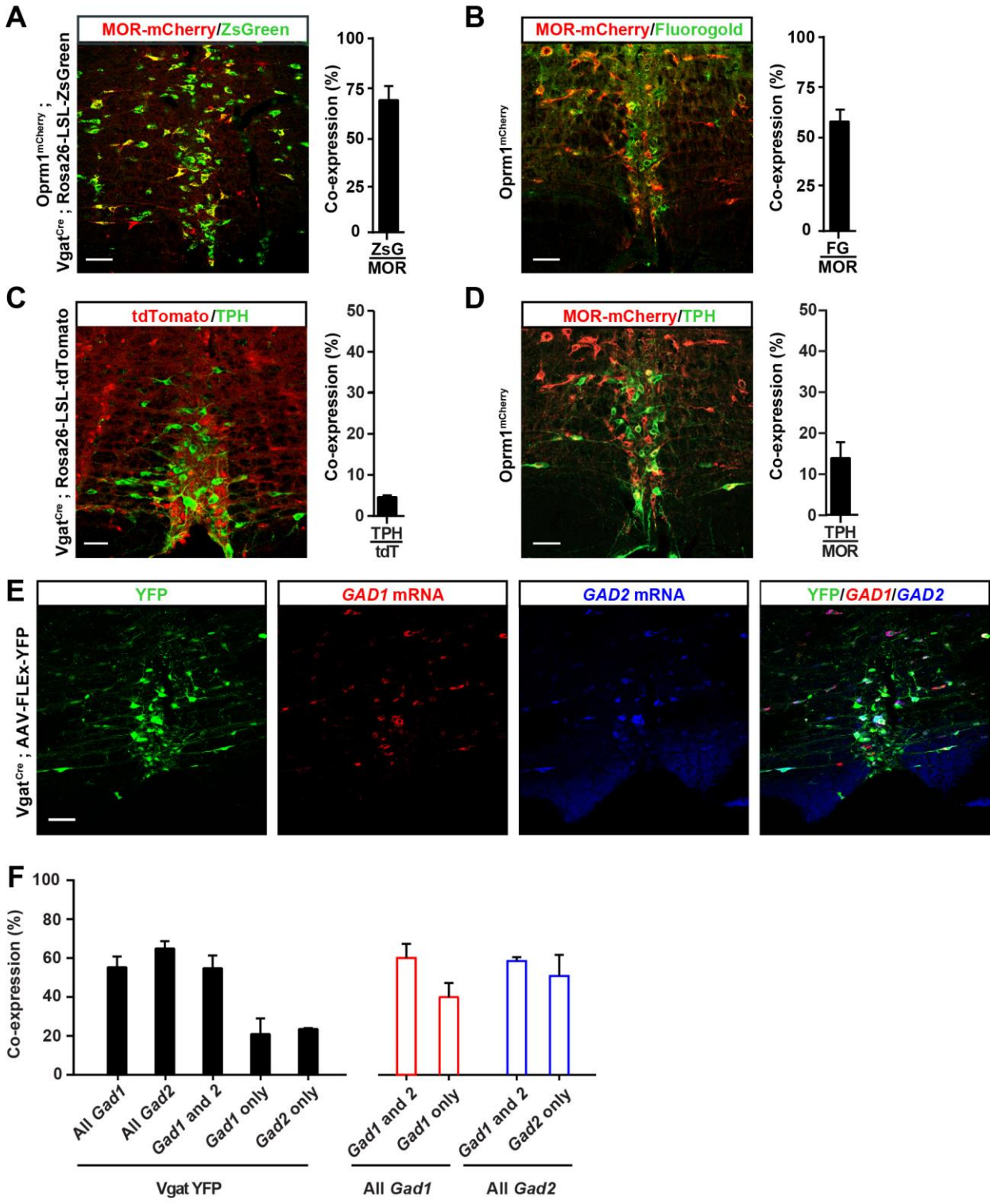
A
MOR-mCherry/ZsGreen
Oprm1mCherry ; Vgat Cre ; Rosa26-LSL-ZsGreen
Co-expression (%)
100
75
50
25
0
ZsG / MOR
B
MOR-mCherry/Fluorogold
Oprm1mCherry
Co-expression (%)
FG / MOR
C
tdTomato/TPH
Vgat Cre ; Rosa26-LSL-tdTomato
50
40
30
20
10
0
TPH / tdT
D
MOR-mCherry/TPH
Oprm1mCherry
TPH / MOR
E
YFP
GAD1 mRNA
GAD2 mRNA
YFP/GAD1/GAD2
Vgat Cre ; AAV-FLEx-YFP
F
Co-expression (%)
100
80
60
40
20
0
All Gad1
All Gad2
Gad1 and 2
Gad1 only
Gad2 only
Gad1 and 2
Gad1 only
Gad1 and 2
Gad2 only
Vgat YFP
All Gad1
All Gad2

Figure S5

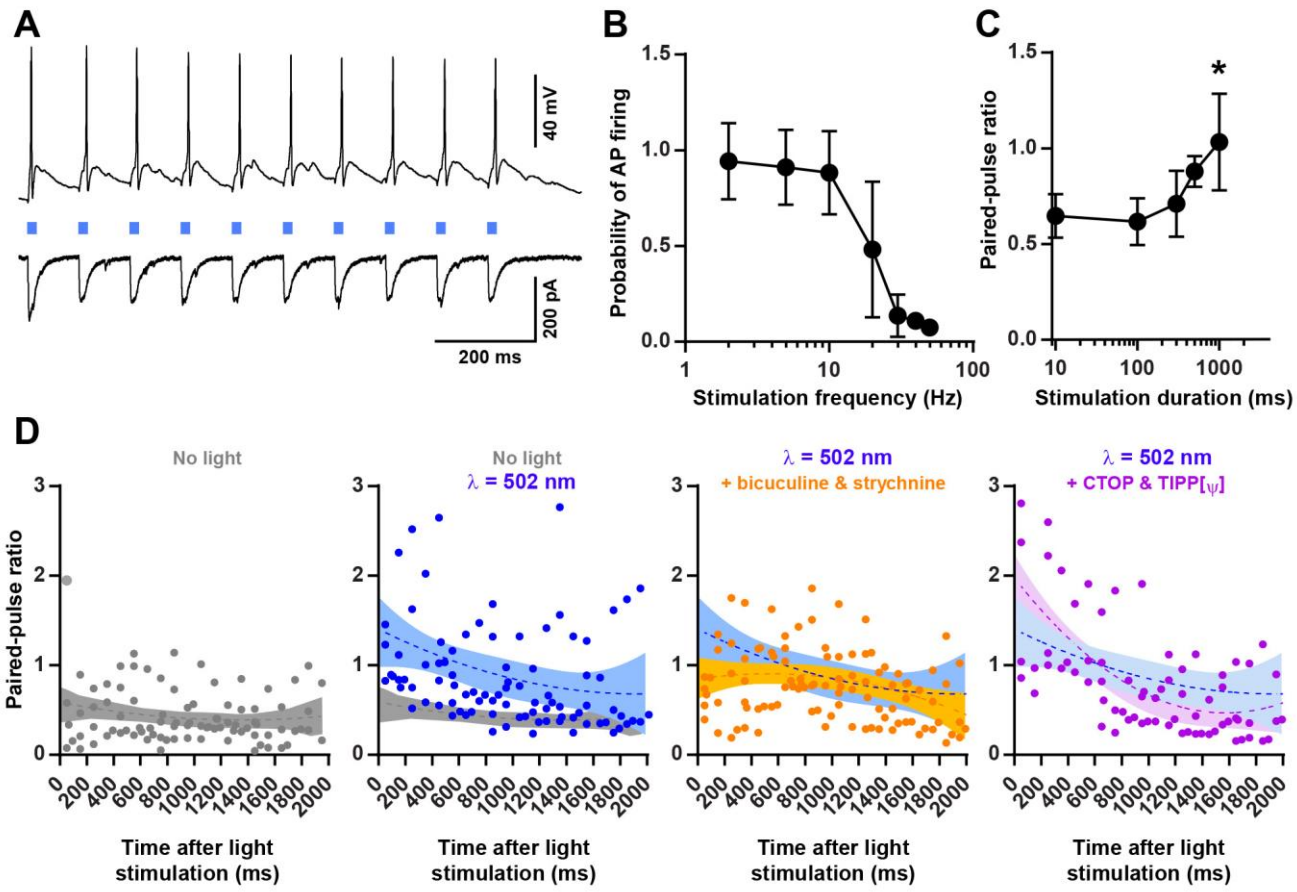
A
40 mV
200 pA
200 ms
B
Probability of AP firing
Stimulation frequency (Hz)
C
Paired-pulse ratio
Stimulation duration (ms)
*
D
No light
No light
λ = 502 nm
λ = 502 nm
+ bicuculine & strychnine
λ = 502 nm
+ CTOP & TIPP[ψ]
Paired-pulse ratio
Time after light stimulation (ms)

Figure S6

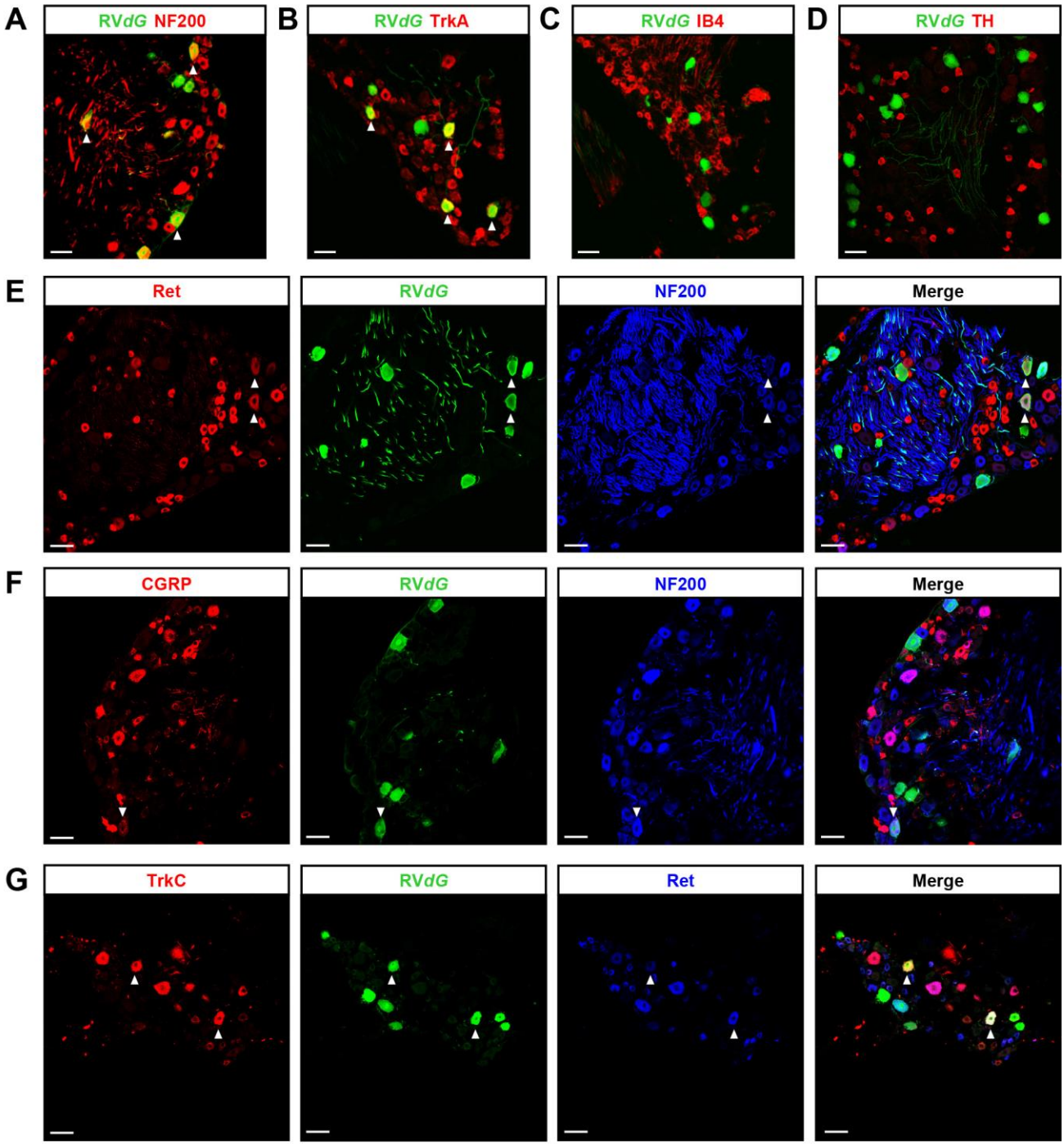
A
RVdG NF200
B
RVdG TrkA
C
RVdG IB4
D
RVdG TH
E
Ret
RVdG
NF200
Merge
F
CGRP
RVdG
NF200
Merge
G
TrkC
RVdG
Ret
Merge

Figure S7

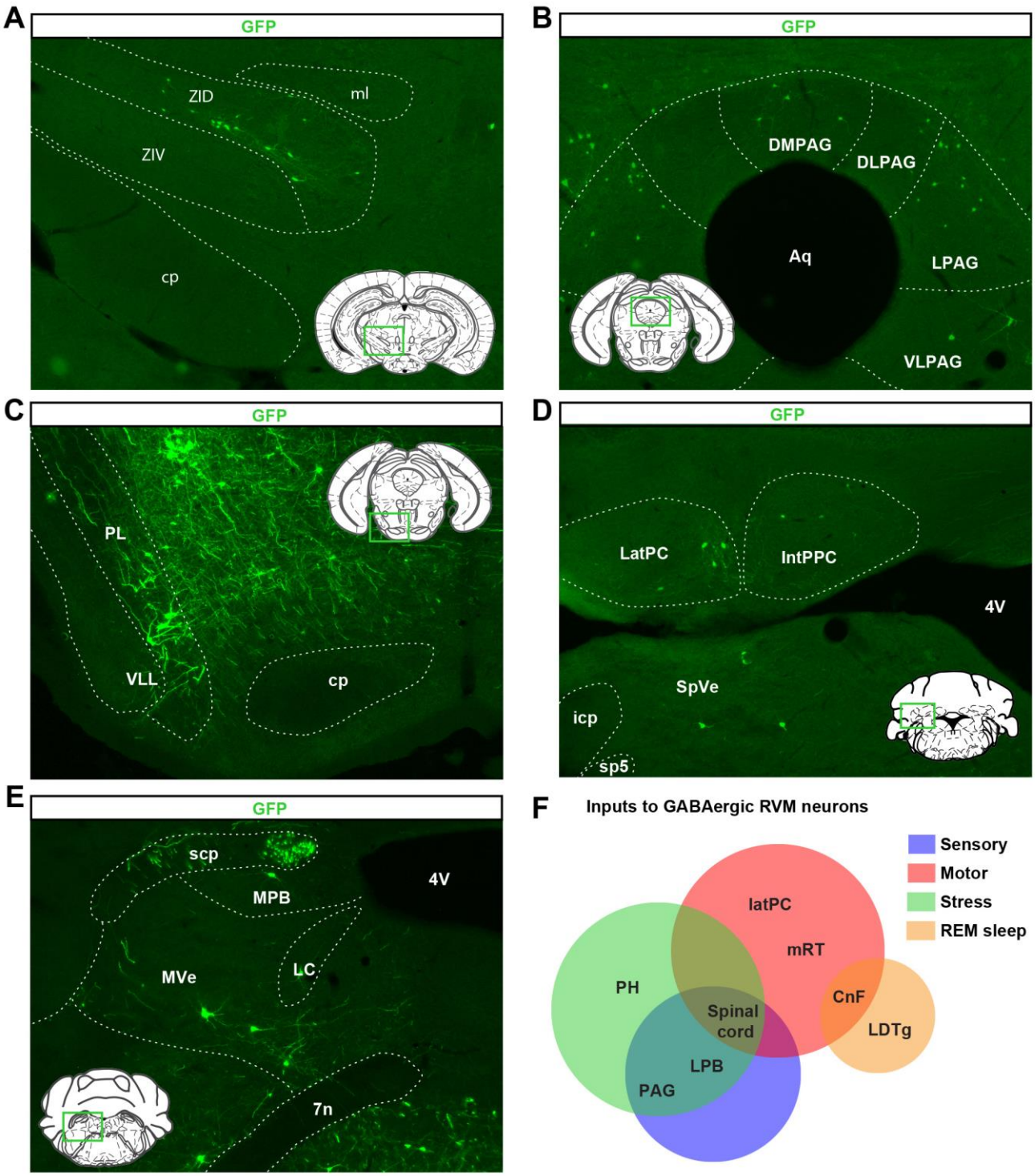
A
GFP
ZID
ml
ZIV
cp
B
GFP
DMPAG
DLPAG
Aq
LPAG
VLPAG
C
GFP
PL
VLL
cp
D
GFP
LatPC
IntPPC
4V
SpVe
icp
sp5
E
GFP
scp
4V
MPB
MVe
LC
7n
F
Inputs to GABAergic RVM neurons
Sensory
Motor
Stress
REM sleep
latPC
mRT
PH
CnF
Spinal cord
LDTg
LPB
PAG

Figure S8

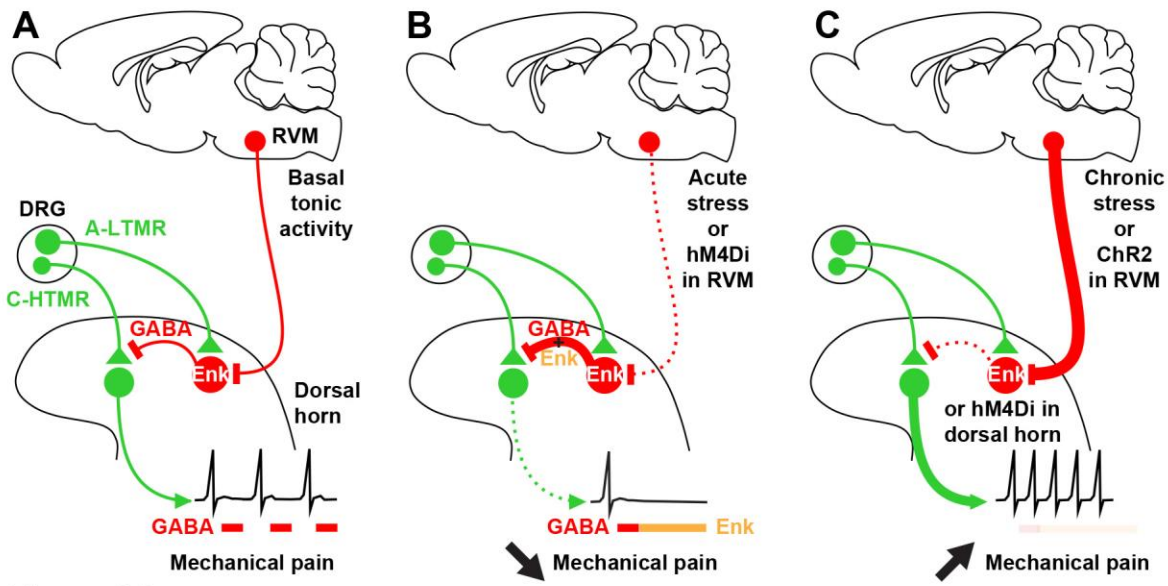

Figure S9

SUPPLEMENTAL FIGURE LEGENDS

Figure S1. Related to Figure 1. Characterization of Penk^{Cre}-expressing spinal neurons using Rosa26-LSL-tdTomato reporter mice.

(**A**) Coronal sections of spinal cord dorsal horn from Penk^{Cre} mice crossed with Rosa26-LSL-tdTomato reporter line. The distribution pattern of tdTomato in Penk^{Cre};Rosa26-LSL-tdTomato mice matches that of *Penk* mRNA in wild type mice.

(**B**) Limited tdTomato and *Penk* mRNA expression in DRG from Penk^{Cre};Rosa26-LSL-tdTomato and wild type mice, respectively.

(**C**) Double fluorescent *in situ* hybridization showing that the majority of Penk^{Cre} tdTomato+ (red) spinal neurons co-express *Penk* (green) (78 ± 1.6%; n=3 mice).

(**D**) Identification of Penk+ neurons by immunohistochemistry. 47±1.2% of Penk^{+} neurons (red) co-express the marker of glutamatergic dorsal horn neurons TLX3 (green; top panels), and 31%±1.7% co-express the marker of GABAergic/glycinergic dorsal horn neurons PAX2 (green; bottom panels).

(**E**) Co-labeling of spinal cord sections from Penk^{Cre};Rosa26-LSL-tdTomato mice with the neuronal marker NeuN (blue), the lamina I/IIo marker CGRP (green, top row), the lamina IIi dorsal marker IB4 (green, middle row), and the lamina IIi ventral/III marker PKCγ (green, bottom row) showing that Penk+ neurons are evenly distributed in the dorsal horn.

(**F**) CNO administration did not alter the latency for paw withdrawal in the sticky tape test in Penk^{Cre} mice expressing hM4Di-mCherry in Penk+ neurons of the right dorsal horn (n = 5).

(**G**) CNO did not change withdrawal responses in the cotton swab test (n = 5).

(**H**) *In situ* hybridization for *Penk* mRNA in the RVM of Penk^{Cre} mice infected with AAV helpers and RV*d*G in the dorsal horn shows that *Penk* is rarely expressed in RVM neurons projecting to spinal dorsal horn enkephalinergic neurons (6.54%±1.62 n=3). Scale bars equal 50 μm. All bar graphs represent mean ± s.e.m.

Figure S2. Related to Figure 1. hM4DI expressed in spinal Vgat neurons and intrathecal bicuculline partially reduce both mechanical and heat sensitivity

(**A**) Systemic injection of CNO in Penk^{Cre} and Vgat^{Cre} mice injected with AAV-FLEx-hM4Di-mCherry in the dorsal horn induced mechanical hypersensitivity. Intrathecal (i.t.) injection of bicuculline (1ng) but not naloxone (5μg) mimics Penk^{Cre} and Vgat^{Cre} hM4Di phenotype in C57B6 mice (WT).

(**B**) CNO in Vgat^{Cre} hM4Di mice and i.t. injection of bicuculline in C57B6 mice also induced heat hypersensitivity but not CNO in Penk^{Cre} mice nor i.t. injection of naloxone in C57B6 mice (Mann Whitney test, *p<0.05, ***p<0.001, **** p<0.0001; n=8,9,10,9). All bar graphs represent mean ± s.e.m.

Figure S3. Related to Figure 2. Inhibition of RVM GABAergic neurons decreases mechanical sensitivity but does not affect heat threshold, touch, motor coordination, or locomotor activity.

(**A**) Injection of an AAV into the RVM of Vgat^{Cre} mice to express hM4Di-mCherry in a Cre-dependent manner.

(**B**) and (**C**) CNO caused strong mechanical hyposensitivity in the von Frey test (Two-way ANOVA, Bonferroni post-hoc test, * p<0.05, **p<0.01, ***p<0.001, ****p<0.0001; n=12,9).

(**D**) CNO injection did not change the latency for paw withdrawal in the sticky tape test in Vgat^{Cre} mice expressing hM4Di-mCherry in Vgat+ RVM neurons (n=12).

(**E**) CNO did not alter withdrawal responses in the cotton swab test (n 12).

(**F**) CNO administration did not impact motor coordination in the rotarod test (n = 6).

(**G**) CNO changed neither the velocity nor the travelled distance in the open field test indicating normal locomotor activity (n=6).

Scale bars equal 100 μm. All bar graphs represent mean ± s.e.m.

Figure S4. Related to Figure 2. Inhibition of RVM GABAergic neurons projecting to the spinal cord does not affect heat threshold.

(**A**) Genetic strategy to express hM4Di only in Vgat neurons projecting to the lumbar spinal cord.

(**B**) Inhibition of only Vgat^{Cre}+ neurons projecting to the spinal cord reduces mechanical sensitivity. (Two-way ANOVA, Bonferroni post-hoc test, * p<0.05, **p<0.01; n=5)

(**C**) Inhibition of Vgat^{Cre}+ neurons with AAV-retro (AAV2-retro-FLEx-FlpO) projecting to the spinal cord does not impact heat sensitivity.

(**D**) Expression of AAV-FLEx-eNphR3-p2A-ChR2-YFP in Vgat^{Cre}+ RVM neurons (left panel) and in terminals in the dorsal horn of the spinal cord (middle and right panels). Right panel shows a close-up of the dashed box shown in the middle panel. Arrows indicate examples of RVM Vgat+ terminals.

Scale bars equal 50 μm. All bar graphs represent mean ± s.e.m.

Figure S5. Related to Figure 2. Characterization of Vgat^{Cre} and MOR-mCherry expressing RVM neurons.

(A) through (**D**) Vgat^{Cre} and MOR-mCherry expressing RVM neurons rarely express serotonin.

(**A**) RVM coronal section from MOR-mCherry mouse crossed with Vgat^{Cre};Rosa26-LSL-ZsGreen reporter showing that 67±5.6% of the RVM neurons that express MOR are ZsGreen+ and GABAergic (n=5).

(**B**) A single injection of fluorogold in the lumbar spinal cord was sufficient to label 55±5.5% of MOR-mCherry+ RVM neurons suggesting that the majority of MOR-expressing neurons project to the spinal cord (n=5).

(**C**) Immunostaining showing that in Vgat^{Cre};Rosa26-LSL-tdTomato mice tdTomato+ RVM neurons rarely co-express the marker of serotonergic neurons TPH (4.7±0.4%, n = 3).

(**D**) MOR+ RVM neurons rarely co-express TPH in MOR-mCherry mice (13.8± 3.9%,; n=3).

(**E**) and (**F**) *Gad1* and *Gad2* are mostly expressed together in Vgat^{Cre} + neurons (59%), but Cre+ neurons are also expressed in 21% of neurons expressing *Gad1* only and 24% of neurons expressing *Gad2* only. *Gad1* and *Gad2* are expressed together in most Vgat+ neurons but 40% of *Gad1* neurons don't express *Gad2* and 50% of *Gad2* neurons don't express *Gad1* (n=3).

Scale bars equal 100 μm. All bar graphs represent mean ± s.e.m.

Figure S6. Related to Figure 4. Characteristics of presynaptic inhibition induced by ChR2-YFP stimulation in Penk+ spinal neurons.

(**A**) Example trace showing action potential firing triggered in a Penk^{Cre} ChR2-YFP-expressing dorsal horn neuron with 10 Hz blue light stimulation.

(**B**) The probability to evoke an action potential in response to a blue light pulse is considerably reduced if the stimulation frequency exceeds 20 Hz.

(**C**) The PPR is significantly increased if the blue light train pulse is longer than 1000 ms (Kruskal-Wallis test, *p<0.05).

(**D**) The PPR increased 50 ms after blue light stimulation, an effect that was blocked by 10 μM bicuculline/2 μM strychnine.

Results are represented as mean ± SEM.

Figure S7. Related to Figure 7. Identification of DRG neurons projecting onto enkephalinergic spinal neurons.

(**A**) through (**D**). Immunostaining indicating the molecular identity of GFP-expressing DRG neurons following injection of AAV helpers and RV*dG* in the dorsal horn of $Penk^{Cre}$ mice (as in Figures 1I and 1J). These panels show that some GFP+ DRG neurons express the marker of sensory neurons with myelinated axons NF200 (A-fibers) and the marker of peptidergic nociceptors TrkA, but neither the marker of non-peptidergic C nociceptors IB4, nor the marker of C low-threshold mechanoreceptors TH.

(**E**) Some GFP+ neurons co-express Ret (red) and NF200 (blue), indicating that they might be cutaneous rapidly-adapting A low-threshold mechanoreceptors.

(**F**) Other GFP+ neurons co-expressing CGRP (red) and NF200 (blue) might correspond to myelinated nociceptors.

(**G**) Some GFP+ neurons co-express TrkC (red) and Ret (blue), identifying as Aβ low-threshold mechanoreceptors forming circumferential endings around hair follicles.

Arrows indicate examples of co-expression. Scale bars equal 50 μm.

Figure S8. Related to Figure 8. Identification of inputs to GABAergic RVM neurons projecting to the spinal cord.

(A) through (**E**) Representative images from coronal brain sections of a $Vgat^{Cre}$ mouse injected with FlpO dependent AAV helpers and GFP-expressing RV*dG* in the RVM and the retrograde

AAV-retro expressing FlpO in a Cre-dependent manner in the spinal cord, as in Figure 7. RVM GABAergic neurons receive inputs from the ZI (**A**), PL (**B**) latPC (**C**), LDTg (**D**), and CnF (**E**).

(**F**) Classification and clustering of the inputs to Vgat+ RVM neurons according to the main function of the brain area where their somata are localized, based on the literature (Baker et al., 2010; Basbaum et al., 2009; Bellchambers et al., 1998; Goetz et al., 2016; Heinricher et al., 2009; Miczek and Winslow, 1987; Todd, 2010; Uusisaari and Knopfel, 2011; Van Dort et al., 2015; Zemlan and Behbehani, 1988).

ZID: Zona incerta dorsal part; ZID: Zona incerta ventral part; cp: Cerebellar peduncle; ml: medial lemniscus; VLL: Ventral nu of the lateral lemniscus; PL: paralemniscal nu: LatPC Lateral cerebellar nu, parvicellular part; IntPPC: Interposed cerebellar nu, posterior parvicellular; icp: inferior cerebellar peduncle; sp5: Spinal trigeminal tract; SpVe: spinal vestibular nuMPB: Medial parabrachial nu; scp: Superior cerebellar peduncle; LC: Locus coeruleus; LDTg: Laterodorsal tegmental nu ventral part; MVe: Medial vestibular nu;7n: Facial nerve.

Figure S9. Related to Figures 1-8. RVM GABAergic neurons facilitate pain via a dorsal horn disynaptic inhibitory circuit and are engaged during stress-induced mechanical hypersensitivity.

(A) RVM GABAergic neurons project to the spinal cord dorsal horn and inhibit spinal GABAergic/enkephalinergic neurons (dorsal horn “Enk” red neuron). These Enk. neurons receive inputs from Aβ- and Aδ-low threshold mechanoreceptors (A-LTMRs) and gate mechanical pain by presynaptically inhibiting C-HTMR afferents, as proposed by Melzack and Wall. GABAergic presynaptic inhibition reduces the strength of nociceptive inputs, which may not prevent acute mechanical pain but may interfere with C-fiber action potential discharge leading to pathological hypersensitivity. **(B)** Acute stress may reduce the strength of GABAergic input from the RVM to the spinal cord, and increase excitability of spinal GABAergic/enkephalinergic neurons and release of GABA and enkephalins. Enkephalins cause long lasting presynaptic inhibition of C-

HTMRs and decrease transmission of nociceptive information, resulting in stress-induced analgesia as observed during the fight-or-flight response. Inhibition of RVM Vgat+ neurons using hM4Di mimics this effect. **(C)** Chronic mild stress may increase activity of RVM GABAergic neurons, which results in inhibition of dorsal horn GABAergic/enkephalinergic neurons and pain facilitation following loss of gating of mechanosensory input. This condition can be mimicked by optogenetic excitation of RVM GABAergic descending axons in the spinal cord, or pharmacogenetic inhibition of spinal enkephalinergic neurons using hM4Di.